

## Electronic Supplementary Information

### Direct laser write process for 3D conductive graphite circuits in polyimide

*Bryce Dorin,<sup>\*a,b</sup> Patrick Parkinson,<sup>a,c</sup> and Patricia Scully<sup>a,b</sup>*

*<sup>a</sup>The Photon Science Institute, The University of Manchester, Oxford Road, Manchester, M13 9PL, United Kingdom.*

*<sup>b</sup>School of Chemical Engineering and Analytical Science, The University of Manchester, Oxford Road, Manchester, M13 9PL, United Kingdom.*

*<sup>c</sup>School of Physics and Astronomy, The University of Manchester, Oxford Road, Manchester, M13 9PL, United Kingdom.*

*\*E-mail: [bryce.dorin@manchester.ac.uk](mailto:bryce.dorin@manchester.ac.uk)*

## S1 Beam Profiling

To determine the minimum spot size of the beam ( $w_0$ ) a wafer of crystalline silicon was ablated at different pulse energies following the technique outlined in reference [1]. This technique expresses the spatial energy distribution of a Gaussian beam as

$$E(r) = E_0 \exp(-r^2/w_0^2). \quad (1)$$

$$r^2 = w_0^2 (\ln E_0 - \ln E(r)) \quad (2)$$

Here  $r$  is the measured beam radius and  $E_0$  is the peak fluence at the center of the beam. This equation can then be rewritten as (2). From this it is clear that the minimum spot size may be found by measuring the slope of a semi-log plot of beam radius squared versus  $E_0$ . The beam radius was measured from the ablation spots in the silicon wafer, which are shown in Fig. S1 (a)-(h). In Fig. S1 (i) the experimental data is fit to equation (2), which returns a minimum spot size of  $2.5 \mu\text{m}$  for the beam.

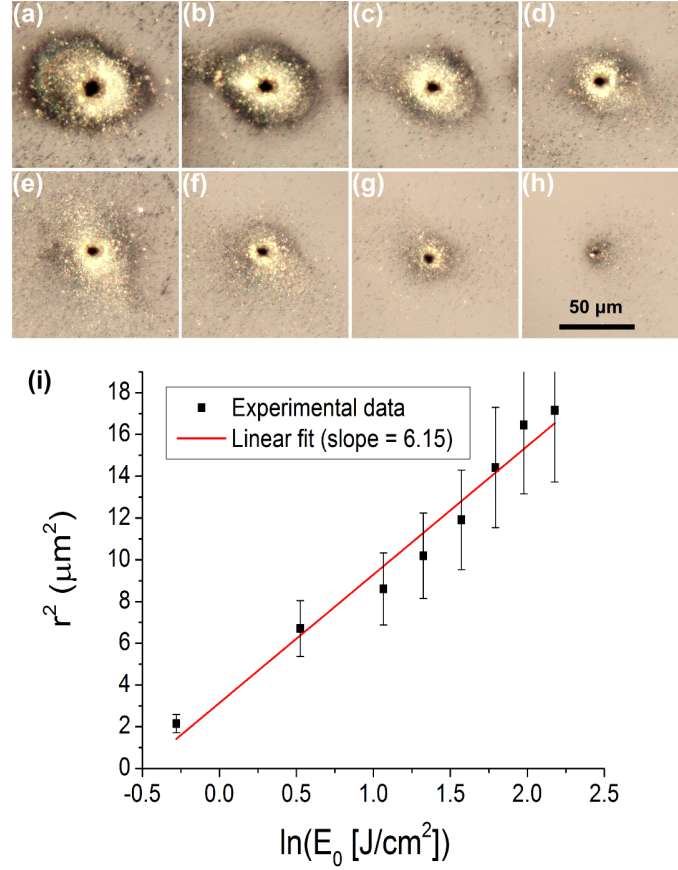


Fig. S1: Microscope images of the ablation of a silicon wafer at pulse energies of (a)  $2.22 \mu\text{J}$ , (b)  $1.82 \mu\text{J}$ , (c)  $1.51 \mu\text{J}$ , (d)  $1.21 \mu\text{J}$ , (e)  $0.95 \mu\text{J}$ , (f)  $0.73 \mu\text{J}$ , (g)  $0.43 \mu\text{J}$ , (h)  $0.19 \mu\text{J}$ . (i) a semi-log plot of the squared ablation radius versus  $E_0$ .

## S2 Absorption spectroscopy

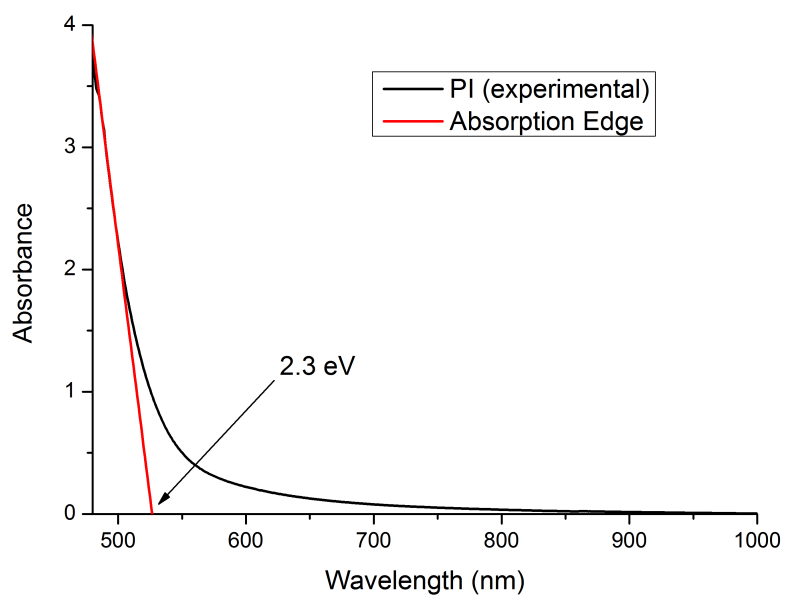


Fig. S2: The absorbance of PI measured on a PerkinElmer Lambda 1050 UV/Vis/NIR Spectrophotometer. The absorption edge was determined to be 2.3 eV.

### S3 Pulse energy dependence

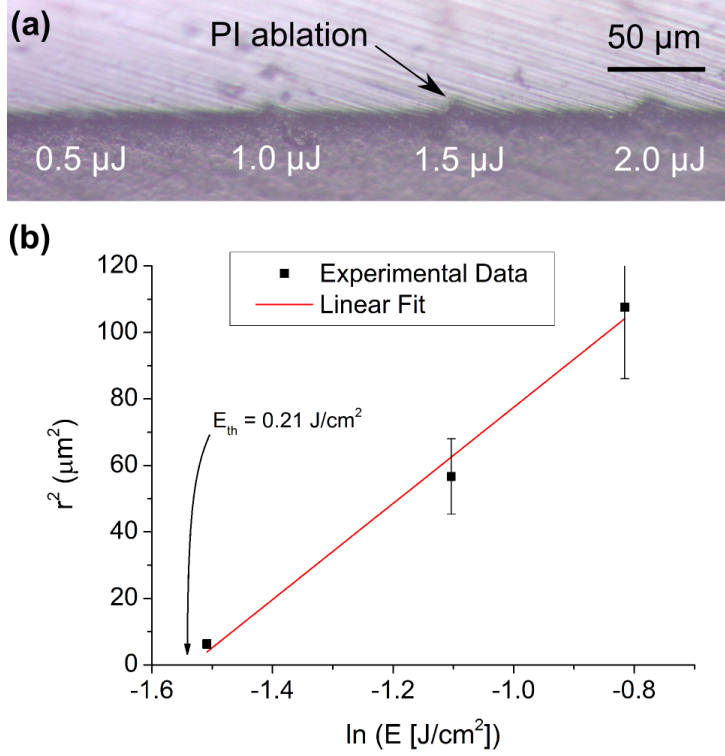


Fig. S3: The pulse energy dependence for ablation of a PI film during DLW at a focus depth of 50  $\mu\text{m}$  below the surface and a scan speed of 10 pulses/ $\mu\text{m}$ . Figure (a) illustrates the surface ablation in the sample cross-section at various pulse energies. In (b) the measured ablation area is plotted as a function of laser fluence. The ablation threshold for the PI film is determined from the X-intercept of a linear fit to this data, which corresponds to a 0.95  $\mu\text{J}$  pulse energy under these conditions.

## S4 Pulse length dependence

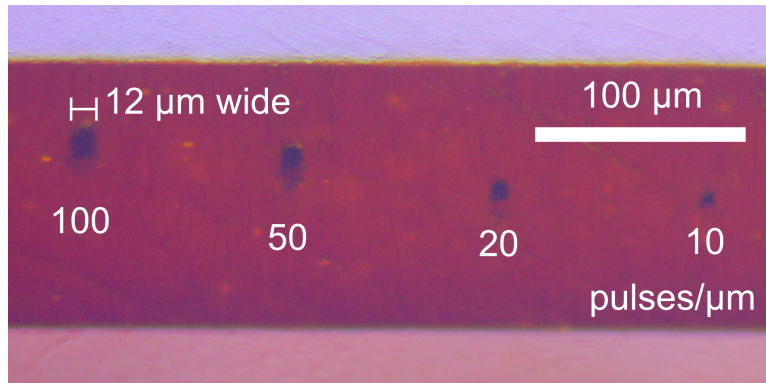


Fig. S4: A microscope image of a cross-sectioned PI film after laser modification at a focal depth of  $40\text{ }\mu\text{m}$  using  $1.5\text{ ps}$  pulses and several scan speeds.

## S5 Mathematical foundation for the thermal model

The temperature rise inside of PI due to the non-linear absorption of femtosecond laser radiation was solved using the three-dimensional heat diffusion equation with a source, which is presented in (3). Here  $D$  is the heat diffusivity of the PI,  $\rho$  is the density, and  $C_p$  is the heat capacity.

$$\frac{\partial T(x, y, z, t)}{\partial t} = D \nabla^2 T(x, y, z, t) + \frac{Q(x, y, z, t)}{\rho C_p} \quad (3)$$

$$Q(x, y, z, t) = Q_0 \exp\left(\frac{-(x - vt)^2 - y^2}{\omega_0^2} + \frac{-z^2}{\omega_z}\right) \sum_{n=1}^N \delta(t - n/f) \quad (4)$$

$$Q_0 = \frac{E\alpha}{\omega_0^2 \omega_z \pi^{3/2}} \quad (5)$$

$Q(x, y, z, t)$  represents the laser heat source [2], which has been expressed in (4). The variable  $v$  represents the speed of the laser scan,  $f$  the number of pulses per second, and  $N$  the number of pulses simulated. The constant  $Q_0$  is the peak power of the beam at the center, which has been solved for in (5) by integrating (4) over all space and equating it to the pulse energy ( $E$ ) multiplied by the non-linear absorbency of the sample ( $\alpha$ ). The length of the pulses are considered to be infinitely small compared to the time-scale for heat diffusion, therefore the time dependant arrival of the pulses is represented using the Dirac delta function,  $\delta$ .

$$\omega_z \simeq z \left( \left[ \frac{\tan(\sin^{-1}(NA/n_1))}{\tan(\sin^{-1}(NA/n_2))} \right] - 1 \right) \quad (6)$$

Variables  $\omega_0$  and  $\omega_z$  represent the size of the beam focus perpendicular and parallel to the beam direction, respectively. In this model the stretching of the focus due to spherical aberrations was accounted for by calculating the refraction of the marginal rays at the air/PI interface [3], as shown in (6). In this equation NA is the numerical aperture of the focusing lens,  $z$  is the nominal focusing depth,  $n_1$  is the refractive index of the initial medium (air), and  $n_2$  is the refractive index of the new medium (PI).

The equation in (3) was solved using the Green's function method [4]. The boundary condition for the problem is that we assume the initial temperature of the sample to be uniform and equal to the room temperature,  $T(x, y, z, 0) = T_0$ . The advantage of the Green's function method is that the formula can

be broken down and solved for each dimension independently first, then combined:

$$G(x, y, z, t|x', y', z', t') = G_x(x, t|x', t')G_y(y, t|y', t')G_z(z, t|z', t'). \quad (7)$$

$$\frac{\partial T(x, t)}{\partial t} = D\nabla^2 T(x, t) \quad (8)$$

$$T(x, t) = \frac{T_0}{\sqrt{4\pi Dt}} \int_{-\infty}^{\infty} \exp\left(\frac{-(x-x')^2}{4Dt}\right) dx' \quad (9)$$

To begin, one must first solve a homogeneous heat diffusion equation in one-dimension [4], as illustrated in (8). The solution to this differential equation is (9).

$$G(x, t|x', t') = \frac{1}{\sqrt{4\pi D(t-t')}} \exp\left(\frac{-(x-x')^2}{4D(t-t')}\right) \quad (10)$$

$$\begin{aligned} T(x, y, z, t) &= \int_{-\infty}^{\infty} \int_{-\infty}^{\infty} \int_{-\infty}^{\infty} G(x, y, z, t|x', y', z', t') T_0 dx' dy' dz' + \\ &\frac{1}{\rho C_p} \int_0^t \int_{-\infty}^{\infty} \int_{-\infty}^{\infty} \int_{-\infty}^{\infty} G(x, y, z, t|x', y', z', t') Q(x', y', z', t') dx' dy' dz' dt' \\ &= T_0 + \sum_{n=1}^N \frac{E\alpha}{\rho C_p \pi^{3/2} (\omega_0^2 + 4D(t-n/f)) \sqrt{\omega_z^2 + 4D(t-n/f)}} \\ &\quad \exp\left(\frac{-(x-tv)^2 - y^2}{\omega_0^2 + 4D(t-n/f)} - \frac{z^2}{\omega_z^2 + 4D(t-n/f)}\right) \quad (11) \end{aligned}$$

Comparing (9) to the definition for the Green's function, one can determine the one-dimensional Green's function (10). Using this same format for the  $y$  and  $z$  components and substituting them into (7), the final solution to (3) can be expressed as (11).

The constants used to solve (11) for the bulk irradiation of PI are summarized in Tab. S1.



Tab. S1: Constants used to solve the heat diffusion model in PI.

Variable	Value	Source
$v$	10 and 5 mm/s	set in stage
$f$	10 000 Hz	set in laser source
$E$	$0.5 \mu\text{J}$	set using optical attenuator
$T_0$	300 K	room temperature
$\alpha$	$0.57 \pm 0.06$	measured during DLW
$\rho$	$1420 \text{ kg/m}^3$	taken from DuPont <sup>TM</sup> Kapton <sup>®</sup> HN Technical Data Sheet [5]
$C_p$	$1090 \text{ J/kg K}$	taken from DuPont <sup>TM</sup> Kapton <sup>®</sup> HN Technical Data Sheet [5]
$D$	$7.75\text{E-}7 \text{ m}^2/\text{s}$	taken from DuPont <sup>TM</sup> Kapton <sup>®</sup> HN Technical Data Sheet [5]
$\omega_0$	$2.5 \mu\text{m}$	measured through beam profiling
$\omega_z$	$50 \mu\text{m}$	calculated using (6) and confirmed experimentally in Fig.1
$n_1$	1.0	refractive index of air
$n_2$	1.7	taken from DuPont <sup>TM</sup> Kapton <sup>®</sup> HN Technical Data Sheet [5]

## S6 Via IV measurements

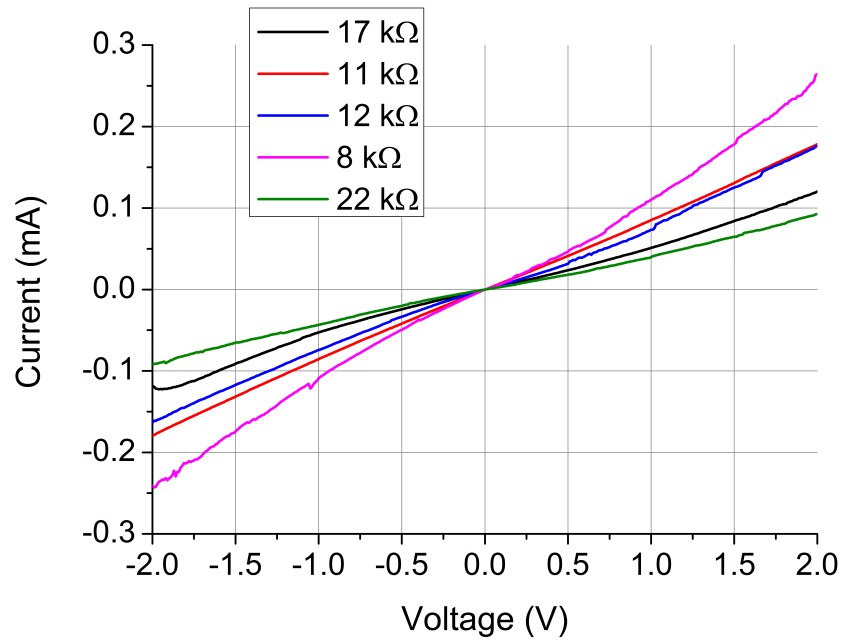


Fig. S5: The IV curves for 5 vias fabricated at 10000 pulses/ $\mu\text{m}$ .

## S7 Electrical turn-on procedure

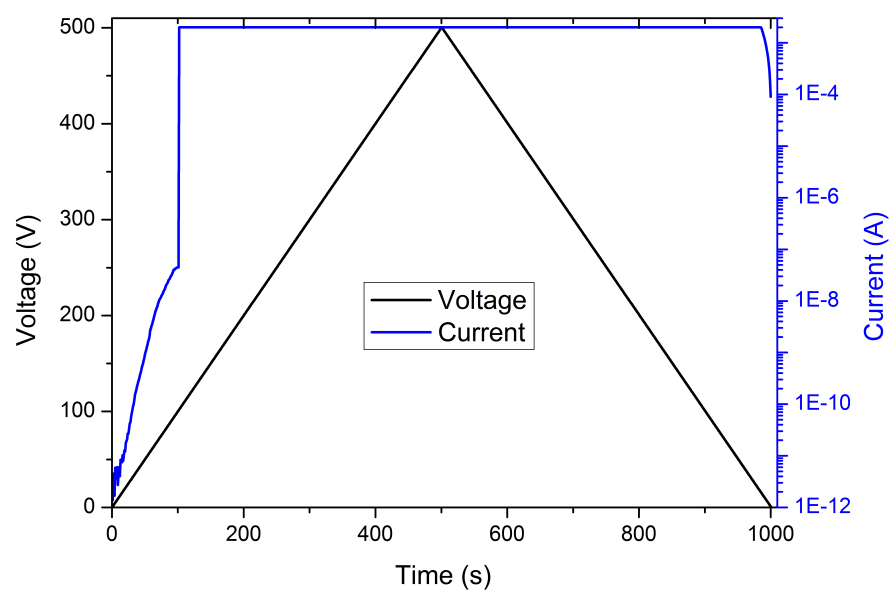


Fig. S6: The turn on of a single DLW via written at 10000 pulses/ $\mu\text{m}$  using a 0–500–0 V sweep. A compliance value of 2 mA is used.

## S8 Electrical stability measurements

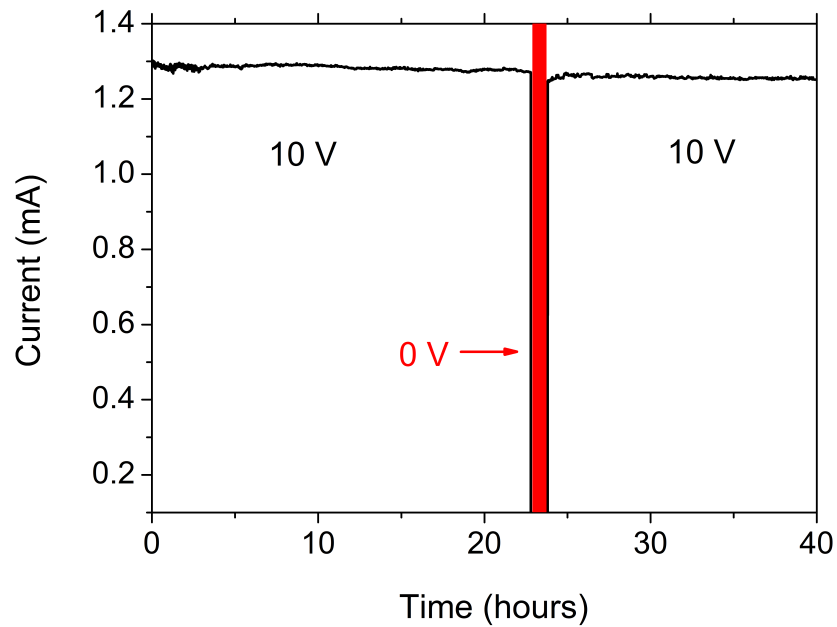


Fig. S7: The current stability of a single DLW via over time and without applied bias. The average current loss was 0.06%/hour.

## References

- [1] Liu, M. J. (1982) *Opt. Lett.* **7**(5), 196–198.
- [2] Wackerow, S. and Abdolvand, A. (2014) *Optics Express* **22**(5), 5076–85.
- [3] Hell, S., Reiner, G., Cremer, C., and Stelzer, E. H. K. (1993) *Journal of Microscopy* **169**(3), 391–405.
- [4] Özisik, M. N. (1993) *Heat Conduction*, John Wiley & Sons Ltd, New York 2nd edition.
- [5] DuPont Technical Data Sheet, Kapton ® HN (2011).